LARGE-ANGLE PROTON NUCLEUS SCATTERING ON ^{208}Pb AND ^{40}Ca

T.E. Drake
Physics Department
University of Toronto
Toronto, Ontario
Canada M5S 1A7

For the past several decades, elastic nucleon-nucleus scattering has been interpreted in terms of phenomenological optical potentials. Calculations using the Schrodinger equation [1], or for that matter the Dirac equation [2], both reproduce the cross section and analyzing power data very well. There are, however, enough parameters in these potentials to ensure that good fits to the data are not difficult to achieve; so agreement with experiment is of limited significance.

There is a current interest in the new microscopic approaches to proton-nucleus scattering. One can regard the "interaction zone" between the incident proton and the nucleus as small compared to nuclear dimension; so at any given point in the nucleus, that bit of nuclear matter can be characterized by its density (Fermi momentum k_F). One can replace the free nucleon-nucleon interaction with the local density approximation (LDA) t-matrix, which includes the effects of the nuclear medium. The optical model potential (OMP) can then be obtained by folding the single-particle density of the target-nucleus ground state with this complex LDA t-matrix. Thus the microscopic optical model potential now has no arbitrary parameters, with the possible exception of the neutron density [3-6]. Figs. 1-3 show a sample of non-relativistic microscopic OMP calculations for comparison with some of the TRIUMF [7] and LAMPF [8] data [5,9,10]. The agreement is indeed remarkable.

More recently, the effective optical model potential,which is 50 MeV deep, has been shown to be a residue of the cancellation of much larger "covariant potential terms", which are of the order of the nucleon mass; thus a relativistic treatment of proton-nucleus scattering appears inescapable [2,11]. Of course, Shakin et al. [12] have already shown that a relativistic Brueckner-Hartree-Fock approach is needed to describe the saturation property of the nuclear matter density; a phenomenon historically regarded in the low-energy, non-relativistic limit. Our calculations have been done using the code DROP3 [13] and Figs. 4-6 show these microscopic calculations for comparison with experiment.

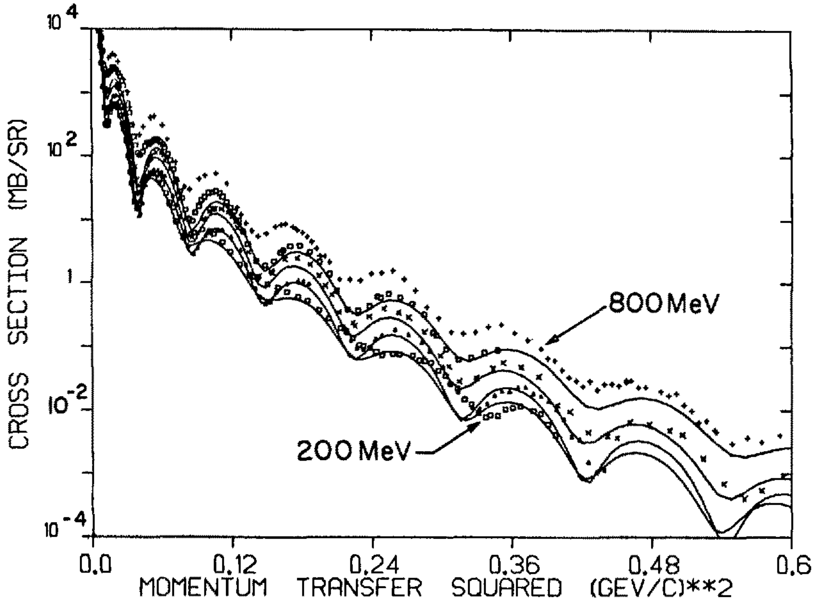

Fig.1 $^{208}Pb(\vec{p},p')$ data for incident proton kinetic energies, $T_p = 200, 300, 400, 500$ and $800 MeV$. The solid curves are MSC calculations using the gauss III densities of Ref. [5].

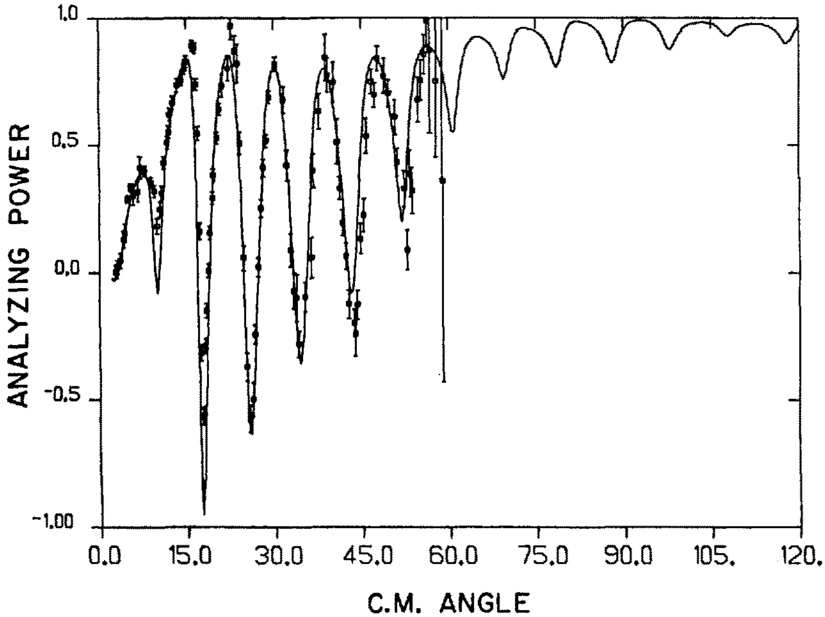

Fig.2 $^{208}Pb(\vec{p},p')$ data for $T_p = 200 MeV$. The solid line is a MSC calculation using gauss III densities.

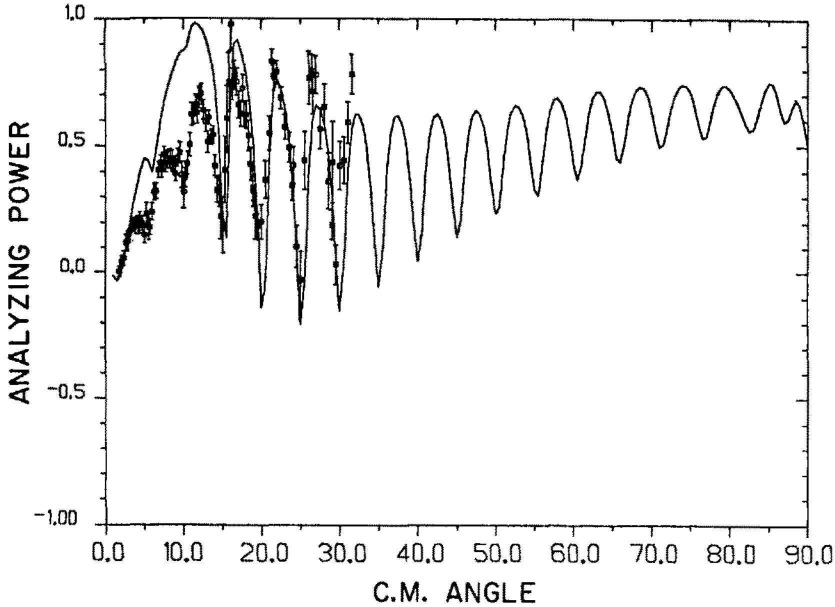

Fig.3 $^{208}Pb(\vec{p},p')$ data for $T_p = 500 MeV$. The solid line is a MSC calculation using gauss III densities.

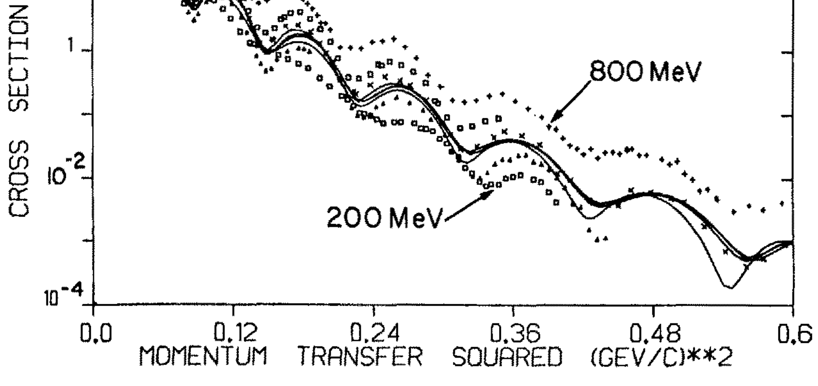

Fig.4 $^{208}Pb(\vec{p},p')$ data for $T_p = 200, 300, 400, 500$ and $800 MeV$. The solid curves are MRIA calculations using gauss III densities.

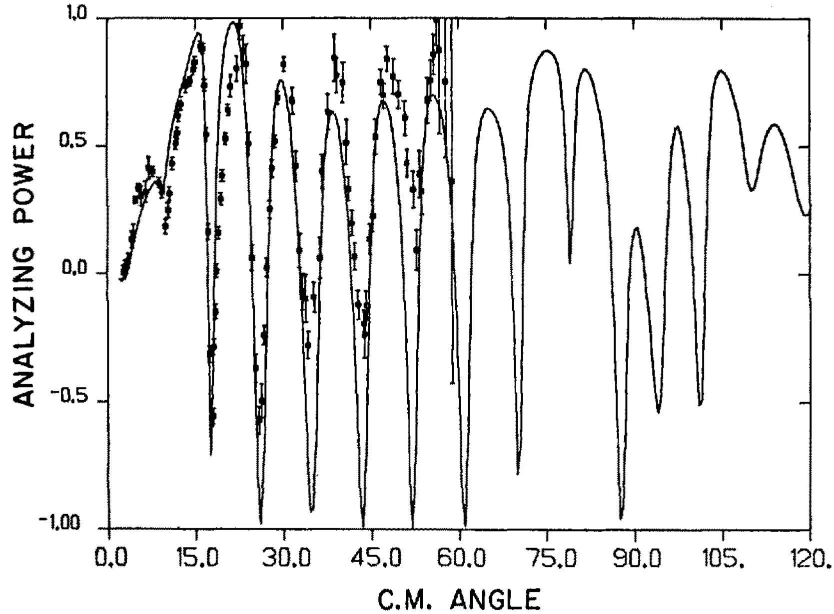

Fig.5 $^{208}Pb(\vec{p},p')$ data for $T_p = 200MeV$. The solid curve is a MRIA calculation using gauss III densities.

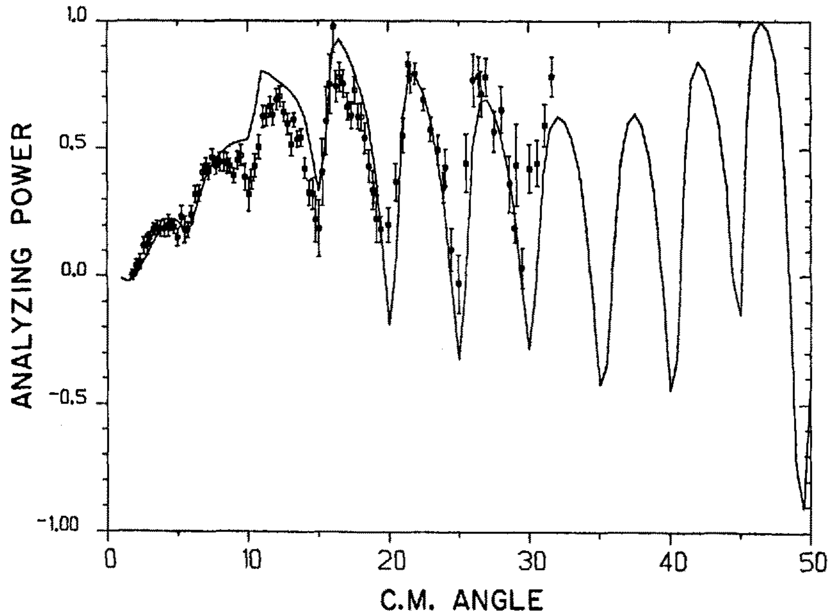

Fig.6 $^{208}Pb(\vec{p},p')$ data for $T_p = 500MeV$. The solid curve is a MRIA calculation using gauss III densities.

The success of the microscopic relativistic impulse approximation [14,15] (MRIA) is evident in the analyzing power and the Q measurements at forward angle, where the effects of the nuclear medium for elastic proton-nucleus scattering are minimal [16,17]. For the analyzing power, a comparison of Figs. 2 with 5 and 3 with 6 shows, that at higher proton kinetic energies, there is a more pronounced difference in the MRIA and the microscopic Schrodinger (MSC) calculations. On the other hand, a comparison of the MRIA calculations of the differential cross section with the world's data on ^{208}Pb reveals a severe defficiency in the MRIA approach, see Fig. 4. It does not reproduce the spread in $\frac{d\sigma}{d\Omega}$ with energy at larger momentum transfer. For the analyzing power, the MRIA and the MSC predictions for 200 MeV proton scattering from ^{208}Pb are presented in Fig. 7. Note how, at large scattering angle, the MSC prediction tends to saturate at $A_y \sim 1$, but the MRIA prediction continues to oscillate about $A_y \sim 0$. The effect of varying the nuclear neutron and proton densities is, of course, greater at larger scattering angle. However, the MSC calculated saturation in A_y is not affected, see Figure 8, and the oscillating nature of the MRIA calculation is also not affected. This large-angle saturation of A_y was first pointed out to the physics community by von Geramb [3], and his work is reproduced in Fig. 9. Indeed, the rest of my talk will concentrate on large-angle proton scattering on ^{208}Pb and ^{40}Ca.

The TRIUMF medium resolution spectrometer (MRS) and beam line 4B have recently undergone a major upgrade [18]. A six quadrupole "twister" was added to beam line 4B for rotation of the beam dispersion from the horizontal to the vertical, to match the MRS. New vertical drift chambers on the focal plane, and new multiwire proportional counters on the front-end, allow ray tracing through the spectrometer. Proton beams with polarization of typically seventy-five per cent and currents of up to one microampere were delivered to 50-100 mg/cm^2 targets of isotopically enriched ^{40}Ca and ^{208}Pb. The beam current on the target was limited only by the event rate in the MRS front-end proportional counters, or by the maximum focal plane rate capability of the data acquisition system, ($\sim$ 400 per second). Beyond the target a large aperture quadrupole doublet was used to refocus the beam into the remote beam dump, and the background was low. At the moment, this facility has an overall resolution of $\sim$ 100-140 keV at 400 MeV [18].

The TRIUMF $^{208}Pb(\vec{p},p')$ elastic data has been extended out to scattering angles of ninety degrees [19], and the differential cross section data is compared to the MSC prediction (solid curve) in Figs. 10 and 11. The analyzing power data is shown in Fig. 12 and the saturation predicted by the MSC calculation (solid curve) follows the data surprisingly well. Indeed, one might also infer from this analyzing power data, that something is missing in the MRIA calculations.

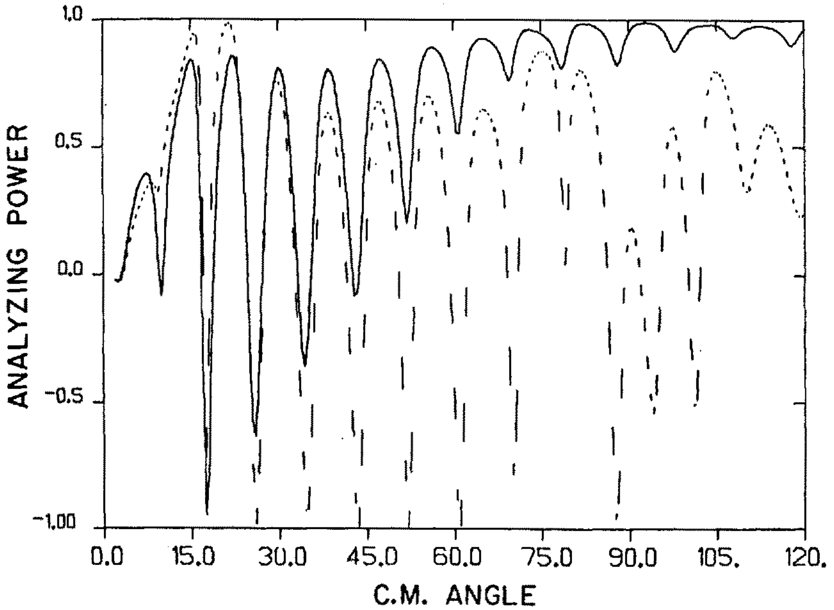

Fig.7 Calculations of A_y for $^{208}Pb(\vec{p},p')$ at $T_p = 200 MeV$, MSC (solid curve) and MRIA (dashed curve) respectively with gauss III densities.

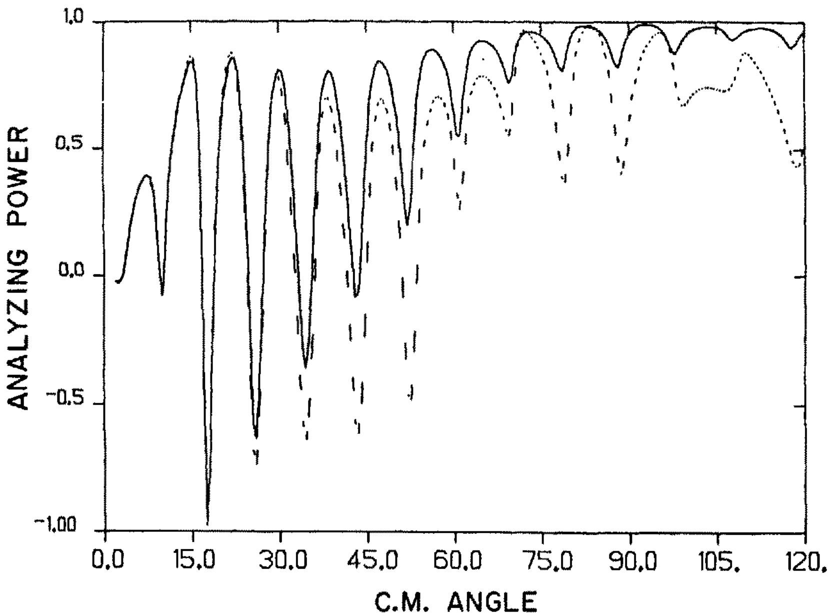

Fig.8 MSC calculations of A_y for $^{208}Pb(\vec{p},p')$ at $T_p = 200 MeV$ using gauss III densities (solid line) and one-body oxford densities [27] (dashed line).

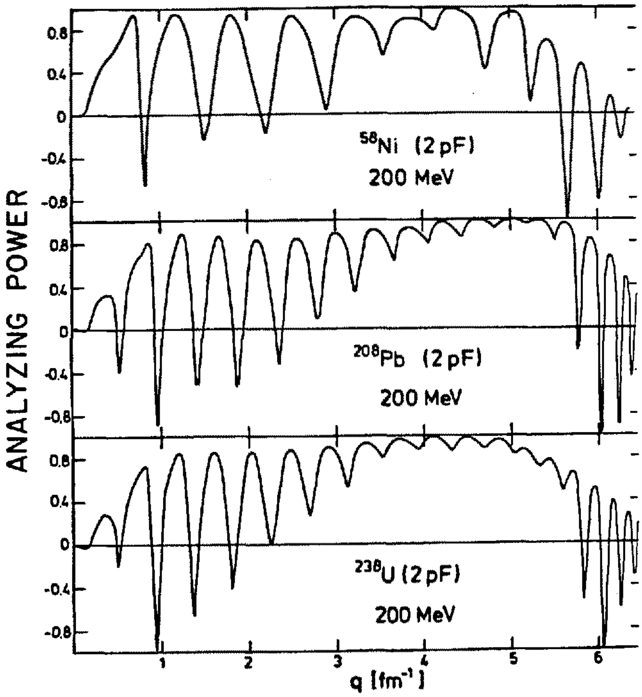

Fig.9 Calculations of A_y for $T_p = 200MeV(\vec{p},p')$ on $^{58}Ni,^{208}Pb$ and ^{238}U taken from Ref. [3].

Brodsky has suggested that the use of the Dirac equation for composite particles is currently an open question; since the nucleon is composite, then the $N - \overline{N}$ pair terms may be strongly suppresed [20]. The ability of the MRIA calculations to predict the analyzing power data at forward angles suggests that the $N - \overline{N}$ pair terms are not suppresed [21]. However, at large scattering angles in ^{208}Pb, the MRIA calculations fail to reproduce the proton kinetic energy dependence of the differential cross section as well as the observed saturation of the analyzing power.

Von Geramb [3] has predicted that the saturation of A_y at large angles will not be observed in lighter nuclei, see Fig. 9. $^{40}Ca(\vec{p},p')$ measurements were made at Triumf and the elastic data are shown in Fig. 13 for a proton kinetic energy of 362 MeV [22].

At IUCF, the large-angle $^{16}O(\vec{p},p')$ measurements at 200 MeV show no saturation effect, and no comparison of this data with microscopic calculations was made. [23].

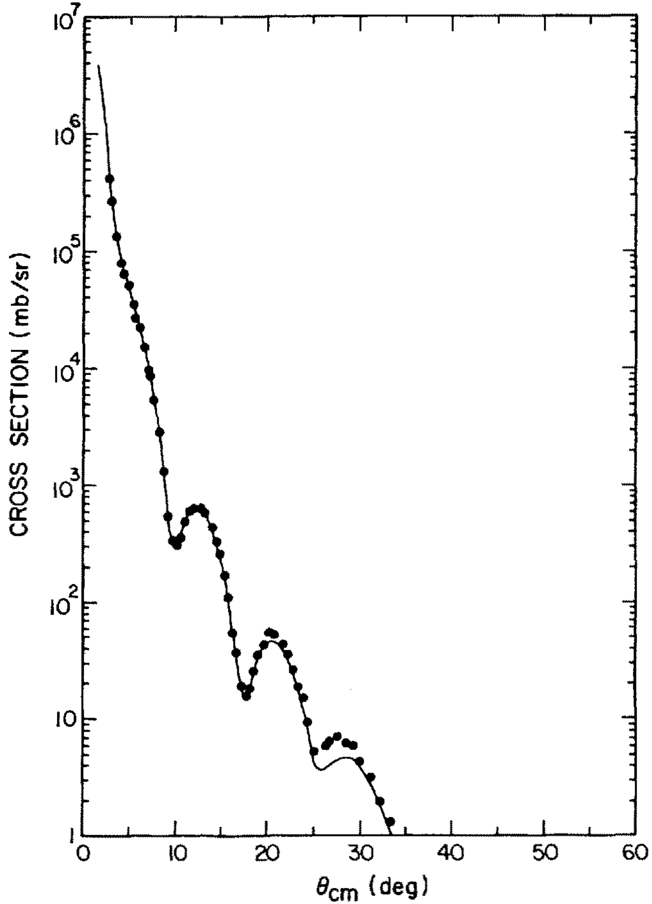

Fig.10 $^{208}Pb(\vec{p},p')$ TRIUMF data [7] for $T_p = 200MeV$. The solid curve is the MSC calculation with gauss III densities.

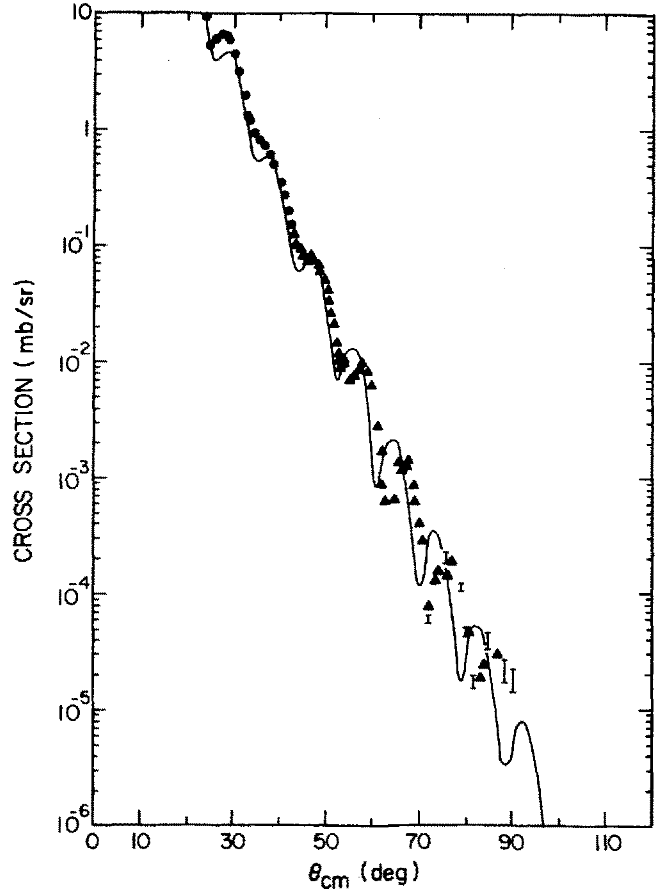

Fig.11 $^{208}Pb(\vec{p},p')$ TRIUMF data for $T_p = 200MeV$. The solid curve is the MSC calculation with gauss III densities. The large angle data is from Ref. [19].

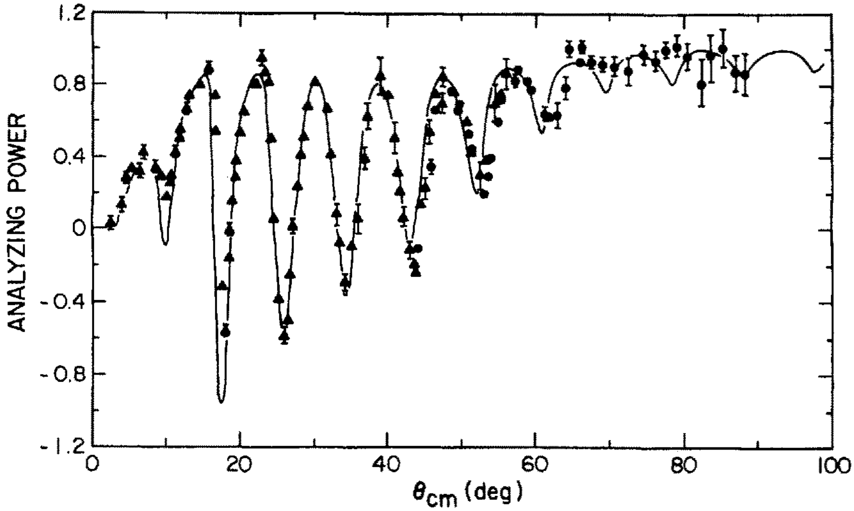

Fig.12 $^{208}Pb(\vec{p},p')$ TRIUMF data at $T_p = 200MeV$. The solid curve is the MSC calculation with gauss III densities. The large angle data is from Ref. [19].

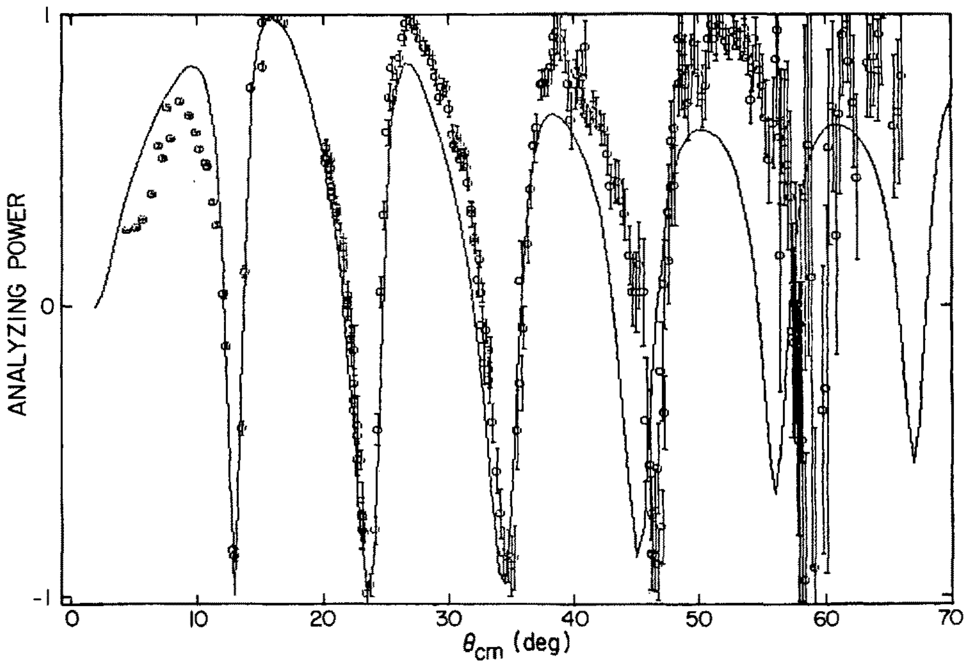

Fig.13 $^{40}Ca(\vec{p},p')$ TRIUMF data [22] at $T_p = 362MeV$. The solid curve is the MSC calculation with one-body densities taken from electron scattering, Ref. [27].

Inelastic proton scattering to natural parity states is known to be a stringent test of microscopic calculations. The transition densities for the different states are localized to different regions of the nuclear surface; so, for example, in the closed-shell nuclei ^{40}Ca and ^{208}Pb, the 5^- states sample the outer nuclear surface but the 3^- and 2^+ states sample the inner surface. The inelastic scattering analyzing powers are known to be especially sensitive to the medium effects. [24-26]. Our Triumf inelastic data for ^{40}Ca and ^{208}Pb were presented to this workshop, but our theoretical calculations for the inelastic data are not yet complete. For the MRIA calculations, the strong covariant scalar and vector potentials may vary as the incoming proton probes deeper into the nuclear surface; their difference may indeed show some suprising effects, and the comparison of theory and experiment for such inelastic data will hopefully provide further insight into the role of "relativity" in nuclear physics.

References

1. P. Schwandt et al.: Phys. Rev. **C26**, 55 (1982); P. Schwandt in *The Interaction Between Medium Energy Nucleons In Nuclei, 1982*, ed. H.O. Meyer, (A.I.P. Conf. Proc. **97**. 1983) page 89.
2. B. Clark et al. in *The Interaction Between Medium Energy Nucleons In Nuclei, 1982* ed. H.O. Meyer, (A.I.P. Conf. Proc. **97**, 1983) page 260.
3. H.V. von Geramb in *Studying Nuclei With Medium Energy Protons,U of Alberta/Triumf Workshop*, ed. J.M. Greben (TRI-83-3, 1983) page 1.
4. H.V. von Geramb in *The Interaction Between Medium Energy Nucleons In Nuclei, 1982* ed. H.O. Meyer, (A.I.P. conf. Proc. **97**, 1983) page 44.
5. L. Rikus, H.V. von Geramb: Nucl. Phys. **A426**, 496 (1984)
6. F.A. Brieva, J.R. Rook: Nucl. Phys. **A291**, 299 and 317 (1977);
   F.A. Brieva, J.R. Rook: Nucl. Phys. **AA297**, 206 (1978)
7. D.A. Hutcheon et al.: Phys. Rev. Letts. **47**, 315 (1981);
   D.A. Hutcheon: private communication.
8. G.W. Hoffman et al.: Phys. Rev. Lett. **47**, 1436 (1981)
9. Hamburg code of H.V. von Geramb, adapted by S.S.M. Wong and R. Dymarz
10. L. Ray: Phys. Rev. **C19**, 1855 (1979)
11. J. McNeill et al.: Phys. Rev. Lett. **50**, 1439 and 1443 (1983)
12. M. Anastasio, L. Celenza, W. Pong, C. Shakin: Phys. Rep. **100**, 327 (1983);
    M. Anastasio, C. Shakin: Phys. Rev. Lett. 45, 2096 (1980)

13. "DROP3", the Dirac equation code of E. Rost, modified by R. Dymarz and S.S.M. Wong.

14. L.S. Celenza et al.: Phys. Rev. **C31**, 63 (1985)

15. M.V. Hynes et al.: Phys. Rev. **C31**, 1438 (1985)

16. L. Ray, G.W. Hoffmann: Phys. Rev. **C31**, 555 (1985) Fig. 17

17. R. Dymarz: Phys. Lett. **152B**, 319 (1985) Fig. 2;
R. Dymarz et al.: Bull. Am. Phys. Soc. **29**, 639 (1984)

18. A. Miller, R. Abegg, S. Yen et al. Triumf preprint, in preparation.

19. A. Miller et al. Triumf; L. Lee et al. Univ. of Toronto; A. Scott et al Univ. of Georgia

20. S.J. Brodsky, J.R. Hiller: Phys. Rev. **C28**, 475 (1983);
S.J. Brodsky in *Short-Distance Phenomena In Nuclear Physics*, eds. Boal, Woloshyn, (NATO ASI Series B104, 1983) page 200.

21. H.J. Weber: Phys. Rev. **C31**, 1476 (1985)

22. D. Frekers et al. Univ. of Toronto; A. Miller et al Triumf.

23. C.W. Glover et al.: Phys. Rev. **C31**, 1 (1985)

24. J. Kelly et al.: Phys. Rev. Lett. **45**, 2012 (1980)

25. W.G. Love in *Studying Nuclei With Medium Energy Protons, Univ. of Alberta/TRIUMF Workshop*, ed J.M. Greben, (TRI-83-3, 1983) page 29.

26. S. Yen et al.: Phys. Lett. **105B**, 421 (1981)

27. J. Streets et al.: J. Phys. **G8**, 839 (1982)